SUBSTRUCTURE ONLINE TEST USING REAL-TIME HYSTERESIS MODELING BY NEURAL NETWORK

Yoshiaki NAKANO[1] and Won-Jik YANG[2]

ABSTRACT: In general, hysteresis models that are applied to a numerical analysis part of substructure online tests do not refer to the experimental behavior of the members/subassemblage under loading tests on a real-time basis. The objective of this study is to develop a new experimental technique for substructure online tests based on nonlinear hysteretic characteristics estimated with a neural network. A new learning algorithm for the network applicable to substructure online tests is proposed, focusing on input layer variables and their normalization method, and its validity is examined through several numerical analytical and experimental investigations. The results show that the new testing scheme successfully reproduces the dynamic behavior of the model structure.

Key Words: earthquake response, substructure online test, neural network, hysteretic characteristics, Ramberg-Osgood model

INTRODUCTION

To date, there have been carried out various experimental researches on seismic performance of structures. Among them, the substructure online test[1-2], also referred to as the hybrid pseudo-dynamic test, has been widely applied to simulate the structural response under earthquake ground motions. The substructure online test is an experimental technique to simulate the earthquake response of an entire structure combining a loading test of the structure's members/subassemblage and a numerical simulation of remaining part of the structure. However, since predetermined mathematical models are generally used in the conventional substructure online tests to represent the hysteretic characteristics of numerical simulation part, they would not take full advantage of the substructure online testing technique unless the behavior of the simulation part is simple or fully understood prior to the online test. The testing technique, therefore, would be enhanced to be applied to more general structures if the online test can be performed without predetermined hysteretic models. To this end, the authors have tried to develop a method to estimate hysteretic characteristics of structural members and its application to the substructure online test, primarily focusing on its formulation through utilizing test results on the real-time basis of the loading test and application of a neural network.

In this paper, the formulation of a neural network which can be applied to the substructure online testing technique is discussed focusing on its structure, learning algorithm, etc. and their validity is investigated through analytical investigations of model structures. To verify the applicability and the effectiveness of the proposed method, four sets of online tests, i.e., (1) the neural network substructure online test (NSOT) newly proposed in this paper, (2) the substructure online test coupled with the

[1] Associate Professor
[2] Cooperative Research Fellow, IIS, University of Tokyo / Research Associate, ESnS Structure Research Center, Kwangwoon University, Seoul, Korea

conventional method (SOT1 and SOT2), and (3) the online test method (OT), are performed and their results are experimentally investigated.

NEURAL NETWORK ALGORITHM

Multilayer feed-forward neural network

In this paper, a multilayer feed-forward neural network[3] is used to estimate the hysteretic characteristics (the load-deflection relationship) of structural members/subassemblage. As shown in Figure 1, the network consists of three layers: an input layer, a hidden layer, and an output layer. As a training algorithm of neural network, the back-propagation method is often applied in previous investigations by other researchers. Studies regarding the network training made by the authors et al.[4], however, revealed that the whole learning method[5] had greater success in saving computation time than the back-propagation method. In this study, the whole learning method is therefore employed as described in subsequent sections.

Random numbers within the range of -0.5 to 0.5 are used as the initial values of the connection weight coefficient. The sigmoid function is used for the transfer function of the input and hidden layers, and the linear function is used for the transfer function of the output layers. The sigmoid and linear functions are shown in Figures 2 and 3, respectively.

Whole learning algorithm

The learning of the feed-forward neural network is classified into a multi-objective optimization problem to minimize the error functions $f^{(n)}$ defined by Eq. (1) for all the training data sets, with respect to the weights associated with the connection between the units, where $O^{(n)}$ denotes the output from the network for the n-th set of the training data, $T^{(n)}$ the corresponding target value, and N the

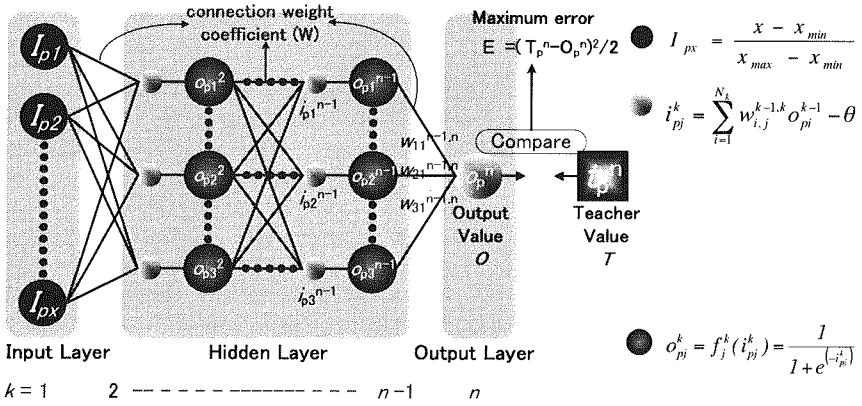

Figure 1. Multilayer feed-forward neural network

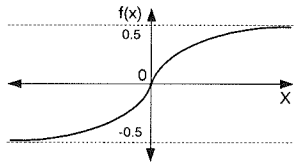

$$f(x) = \frac{1}{1 + exp\,(-x)} - 0.5$$

Figure 2. Sigmoid function

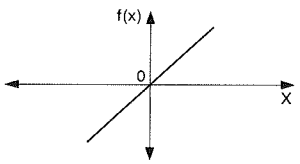

$$f(x) = x$$

Figure 3. Linear function

total number of training data sets.

$$f^{(n)} = \left| T^{(n)} - O^{(n)} \right| \quad (n=1, ..., N) \tag{1}$$

After the Taylor series expansion of $O^{(n)}$ with respect to . W_j, the error function $f^{(n)}$ is approximated by Eq. (2), where J denotes the total number of weights.

$$f^{(n)} = \left| T^{(n)} - \left(O^{(n)} + \sum_{j=1}^{J} \frac{\partial O^{(n)}}{\partial W_j} . W_j \right) \right| \quad (n=1, ..., N) \tag{2}$$

The error function by Eq. 2 can be rewritten with respect to all the training data sets, as shown in Eq. (3).

$$\{f\} = \{b\} - [B]\{\Delta W\} = \{0\} \qquad \{b\} = \left\{ T^{(n)} - O^{(n)} \right\} , \quad [B] = \left[\sum_{j=1}^{J} \frac{\partial O^{(n)}}{\partial W_j} \right] \tag{3}$$

where $[B]$ is the $N \times J$ rectangular matrix of coefficients, $\{b\}$ is the constant vector of N components, and $\{. W\}$ is the unknown variable vector. The solution of the unknown variable vector $\{. W\}$ is determined by using the Moore-Penrose generalized inverse[6], as shown in Eq. (4).

$$\{\Delta W\} = [B]^{-} \{b\} \qquad [B]^{-} : \text{Moore-Penrose generalized inverse} \tag{4}$$

Structure of neural network

The structure of the multilayer feed-forward neural network is shown in Table 1. In this study, two cases of input layers, Input Layer A and B, are investigated as shown in Table 1. The Input Layer A[7] has five variables of (1) maximum displacement, (2) maximum restoring force, (3) displacement at latest turning point, (4) restoring force at latest turning point, and (5) current displacement. It should be noted that variables (1) through (4) are determined over the range of loading steps 1 to i-1, while the variable (5) is corresponding to the current loading step i. The Input Layer B has (1) maximum turning displacement, (2) maximum turning restoring force, and other 3 variables that are the same as (3) through (5) of Layer A.

Since there is no clear standard to determine the appropriate number of nodes in the hidden layer, this study introduces the algorithm studied by Joghataie[8] et al. The hidden layer starts with 5 nodes which are the same number as the input layer, and the number of nodes automatically increases as learning is repeated, as will be described later in detail. The output value, i.e., the estimated results with the neural network, is the restoring force corresponding to the current displacement (input variable (5)) for both cases of Layers A and B.

Normalization of input layer variables

All data to be learned are generally given prior to learning of the multilayer feed-forward neural network, and they are usually normalized with the known minimum and maximum values of each variable in the input layer (conventional method). Since the number of input data N to be learned herein, however, increases as the loading test progresses, the minimum and maximum values of the response can not be determined prior to the online test. In this study, two normalization methods are proposed and their applicability to online tests is investigated as well as the conventional method.

Investigated are the following 3 normalization methods, i.e., (a) Conventional Method, (b) Method I, and (c) Method II. The minimum point ($X1'$, $P1'$) and the maximum point ($X2$, $P2$) on the load-deflection curve are normalized in the following manner.

(a) Conventional Method: Each variable within ($X1'$, $P1'$) to ($X2$, $P2$) is normalized over the range of

[-0.5, 0.5] depending on its minimum and maximum values as shown in Figure 4(a).

(b) Method I: Each variable is subdivided into a displacement group (variables (1), (3), and (5) in Table 1) and a restoring force group (variables (2) and (4) in Table 1). A symmetric range of [*-X2, X2*] for the displacement group and [*-P2, P2*] for the restoring force group is set [-0.5, 0.5], respectively, and data in each group are then normalized over the range of [-0.5, 0.5] as shown in Figure 4(b).

(c) Method II: Each variable is subdivided into two groups and a symmetric range of displacement and restoring force is set [-0.5, 0.5] as is done in Method I. Note that a symmetric range of $[-\overline{P2}, \overline{P2}]$ instead of [*-P2, P2*] is used for the restoring force group, where $\overline{P2}$ is obtained using the initial

Table 1. Structure of neural network

Input Layer	A	(1) Maximum displacement ($\|X_{i-1}\|_{max}$) (2) Maximum restoring force ($\|P_{i-1}\|_{max}$) (3) Displacement at latest turning point (X^t) (4) Restoring force at latest turning point (P^t) (5) Current displacement (X_i)
	B	(1) Maximum turning displacement ($\|X^t_{i-1}\|_{max}$) (2) Maximum turning restoring force ($\|P^t_{i-1}\|_{max}$) (3) Displacement at latest turning point (X^t) (4) Restoring force at latest turning point (P^t) (5) Current displacement (X_i)
Hidden Layer		One layer, starting with five units
Output Layer		Current restoring force

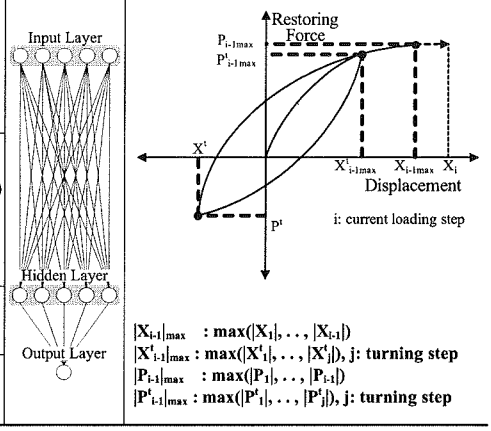

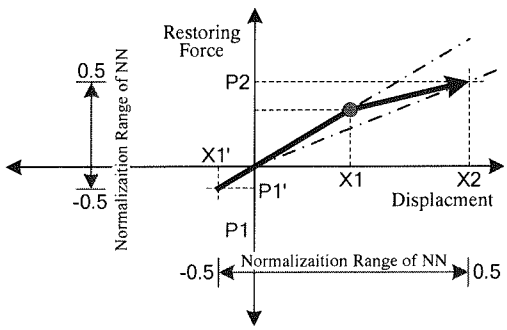

(a) Conventional method

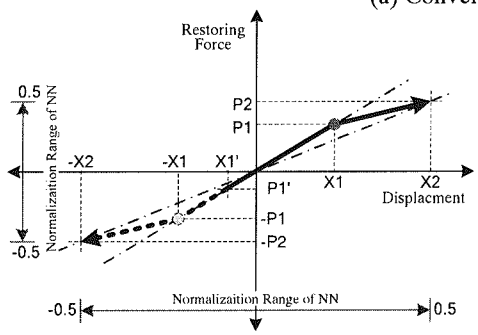

(b) Method I

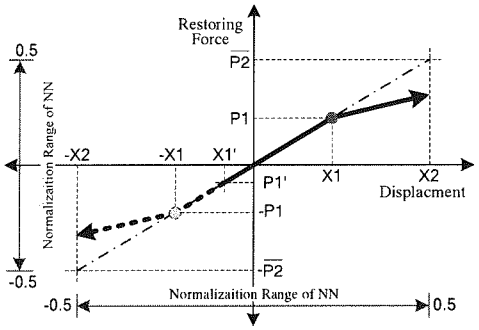

(c) Method II

Figure 4. Normalization method

stiffness and the displacement *X2*. Data in each group are then normalized as shown in Figure 4(c) following the Method I described above.

The normalization above is made repeatedly when the maximum displacement is updated. Note that the normalization methods I[9] and II are introduced to re-normalize data less frequently than the conventional method, and eventually are expected to result in shorter computation time. In particular, the method II is expected to have much shorter computation time due to less frequent re-normalization of restoring force than other two normalization methods.

EARTHQUAKE RESPONSE ANALYSIS USING NEURAL NETWORK

Model structure and investigated parameters

Numerical analyses are conducted to investigate the applicability of the real-time hyteresis modeling with neural network to substructure online tests. A prototype building shown in Figure 5(a) is studied in two cases. In the first case RR, the hysteretic rule of the first and second story is represented by the Ramberg-Osgood model as shown in Figure 5(b). In the second case RN, as can be seen in Figure 5(c), the first story is represented by the Ramberg-Osgood model, while the second story is estimated by the neural network that learns the hysteretic characteristics of the first story on real-time basis.

In the RN analysis, two types of input layer A and B shown in Table 1, and three types of normalization methods shown in Figure 4, are considered as is shown in Table 2. The responses of RN model are then compared with those of RR model, which is deemed to have correct target responses. It should be noted that in the case of RN, the predicted restoring force at the current step i is fed back to define the input variables (2) and (4) shown in Table 1 in the subsequent computation step i+1.

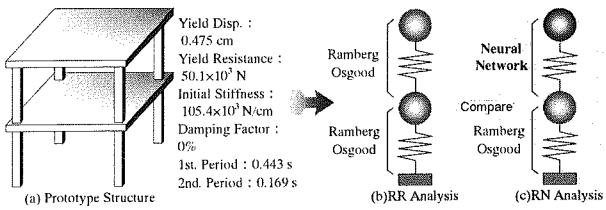

Figure 5. Modeling of structure

Table 2. Parameter of analyses

Analysis	Input Layer	Normalization
RR Analysis	**Target Response**	
RN Analysis	RN - A (Input layer A)	**Conventional Method (Fig. 4(a))**
	RN - B (Input layer B)	
RNI Analysis	RN I-A (Input layer A)	**Normalization Method I (Fig. 4(b))**
	RN I-B (Input layer B)	
RNII Analysis	RNII-A (Input layer A)	**Normalization Method II (Fig. 4(c))**
	RNII-B (Input layer B)	

Numerical integration and input earthquake ground motion

The OS (Operator Splitting) method[1] is used for numerical integration of earthquake response analyses, and the time interval of the integration is set 0.01 second. Since the assessment of the earthquake response of a specific building is not the main purpose herein, the damping effects are neglected in the analyses. For the input earthquake ground motions, used is an accelerogram for 20 seconds (a total of 2000 steps) including major motions of the NS component of the Chiba-ken Toho-oki earthquake recorded in 1987 at the Chiba Experiment Station of the Institute of Industrial Science, University of Tokyo, Japan.

Convergence conditions

In the nonlinear earthquake response analyses using the neural network hysteresis prediction technique, the prediction error is defined as $[T^{(n)} - O^{(n)}]^2 / 2$, and learning is made (maximum 100 times in 1 trial) under its allowable error of 10^{-4}. If the error is still larger than the allowable after 100 time learning, the pattern of initial connection weight coefficient (w) of the neural network is re-normalized based on the current learning results, and the learning procedure is re-performed. This procedure is repeated up to 20 trials. If the solution does not fall within the allowable error range after 20 trials, one more node is added in the hidden layer, and the same procedure (maximum 20 trials with 100 time learning in

each trial) is again repeated. Since this study aims to apply a neural network to the substructure online test, it is favorable to avoid spending too much time for determining the network structure. Considering the previous research result[3], the number of nodes in the hidden layer is therefore limited to 12 (the number of nodes in the hidden layer may change within the range of 5 through 12), and the allowable error is increased from 10^{-4} to 10^{-3} if a satisfactory solution is not obtained until the number of nodes reaches 12. Furthermore, to reduce the learning time, learning is conducted in each response computation until the input acceleration attains the maximum value (PGA), and then learning after PGA is made only when the maximum response displacement is updated.

Analysis results

The computed results are compared in Figures 6 through 8, and the time spent for the analyses is summarized in Table 3(CPU: Pentium IV, Xeon 1.4 GHz, 3650 Mflops), where most of the time is spent for network learning rather than response computation.

The case RN-A poorly reproduces the response and the computation is terminated at 900th step after 8 hours due to a large prediction error, while RN-B has fairly good agreement with RR results although the computation spends approximately 11 hours. RN II series show excellent predictions and much shorter computation time than RN and RN I series. As is found in Table 3, RN II-A shows 1/5 of RN I-A, and RN II-B shows 1/3 of RN I-B in computation time. These results suggest that the

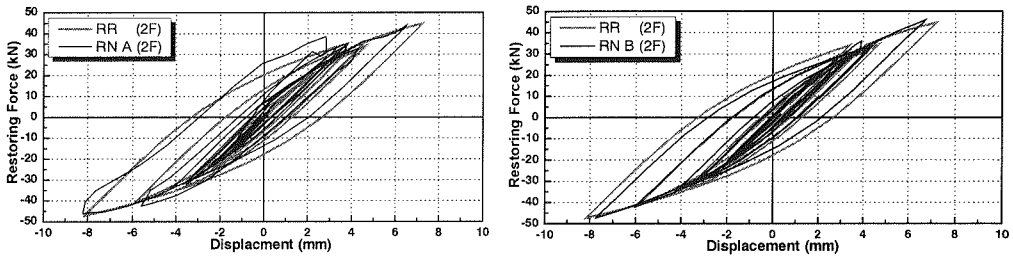

(a) 2nd story by RN-A (b) 2nd story by RN-B

Figure 6. Predicted earthquake response using conventional normalization method

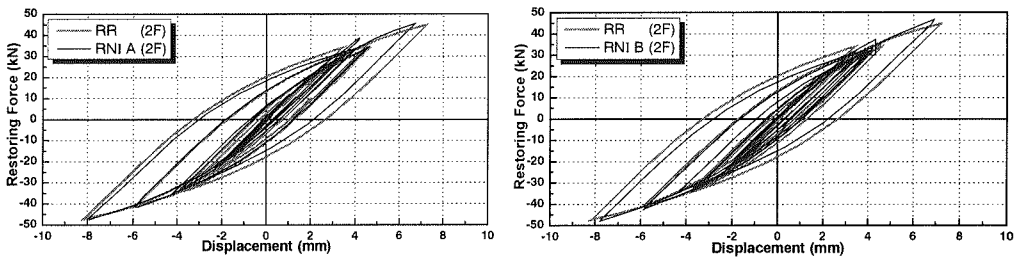

(a) 2nd story by RN I-A (b) 2nd story by RN I-B

Figure 7. Predicted earthquake response using normalization method I

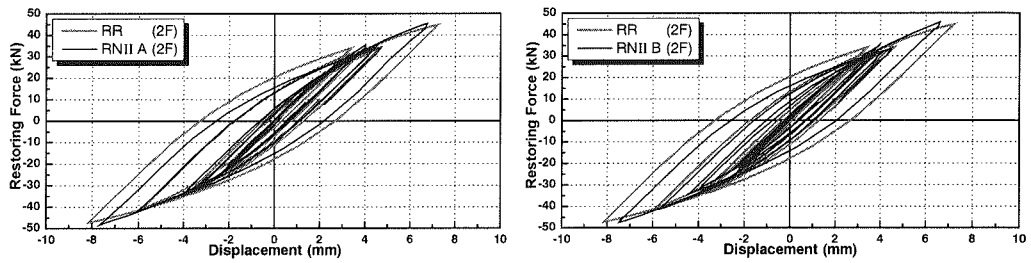

(a) 2nd story by RN II-A (b) 2nd story by RN II-B

Figure 8. Predicted earthquake response using normalization method II

Table 3. Computation time and number of nodes [CPU : Xeon 1.4 G, 3659 Mflops]

Analysis Type	Maximum Number of Hidden Layer Nodes		Computation Time (h:m:s)	Maximum Error*	Computation Ended Step
RN Analysis	RN - A (Input layer A)	12	Approx. 8 hrs	-	900th step
	RN - B (Input layer B)	12	Approx. 11 hrs	0.968	2000th step
RN I Analysis	RN I-A (Input layer A)	12	04:09:00	0.968	2000th step
	RN I-B (Input layer B)	12	03:03:00	0.968	2000th step
RN II Analysis	RNII-A (Input layer A)	6	00:46:01	0.450	2000th step
	RNII-B (Input layer B)	8	00:59:26	0.545	2000th step

*** Error at computation ended step: $[T^{(n)}\text{-}O^{(n)}]^2/2$ ($\times 10^{-3}$).**

proposed normalization method II can be a promising candidate for its application to the substructure online test.

NUMBER OF PREDICTED MEMBERS AND ITS INFLUENCE ON RESPONSE ESTIMATION

In the previous section, a simple two story structure is investigated, where the neural network prediction is applied only to the second story. The response, however, may be less satisfactorily reproduced due to prediction error accumulation when the number of members to be predicted with the neural network increases. In this section, the responses of 3 model structures are further investigated, and the influence of number of members predicted with the neural network is examined focusing on its prediction accuracy.

Model structures and investigated parameters

Figure 9 shows the investigated 3 model structures. They are 4-story, 8-story, and 12-story buildings, and each model is assumed to have identical structural characteristics in each story that are all the same as the 2-story model described earlier in Figure 5. The earthquake response of each model is computed in two cases, RR and RN analysis, likewise the previous 2-story model. Each story is characterized by the Ramberg-Osgood model in RR analyses (target response), while the first story is represented by the Ramberg-Osgood model and the upper stories are estimated by the neural network in RN analyses. In RN analyses, the normalization method II is employed and two input layers, Layer A and Layer B, are investigated under the method II, and their results are compared with those of RR analyses. Input ground motions, learning algorithm, and other fundamental parameters are the same as the 2-story model case.

Analysis results

Figure 10 compares the responses by RR analyses and RN analyses, together with the envelope curve of the first story learned by the neural network. In each figure, a satisfactorily predicted result is shown in the upper figure, while a poorly predicted is shown in the lower. The time history of response displacement for the 3rd story of 8-story model, which is the most poorly predicted result in this study under Input Layer B, is shown in Figure 11.

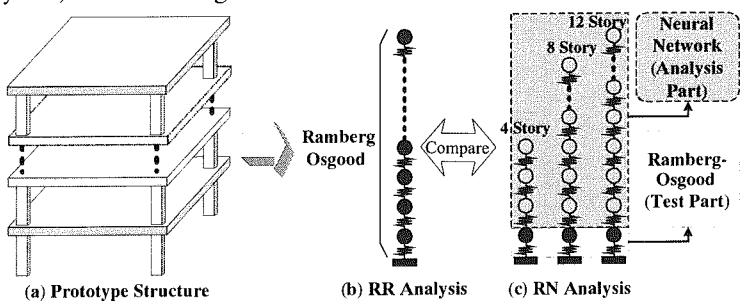

Figure 9. Structure modeling

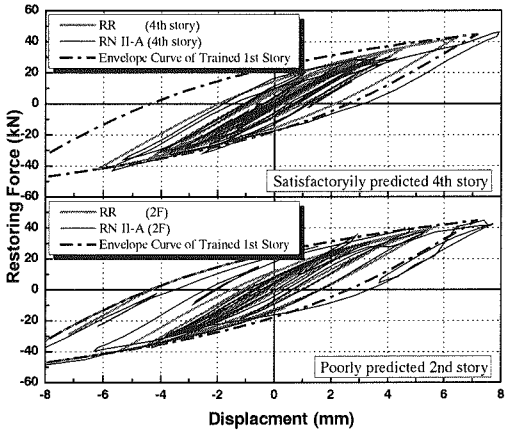

(1-A) 4-story model by RN II-A

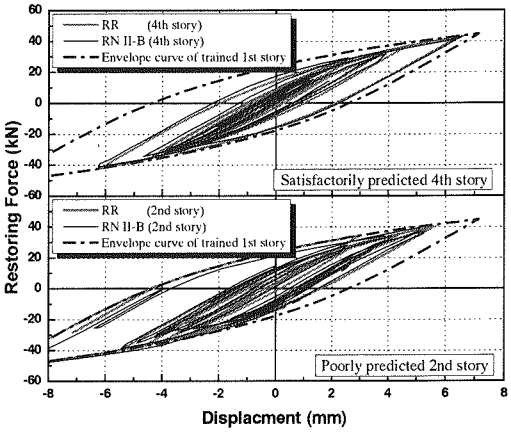

(1-B) 4-story modelby RN II-B

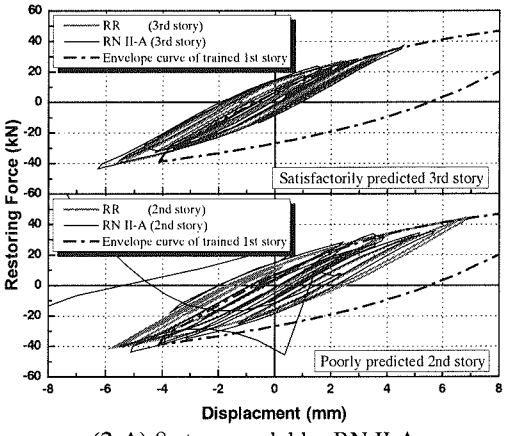

(2-A) 8-story model by RN II-A

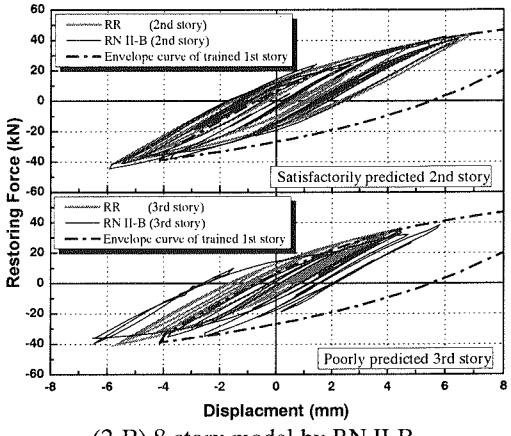

(2-B) 8-story model by RN II-B

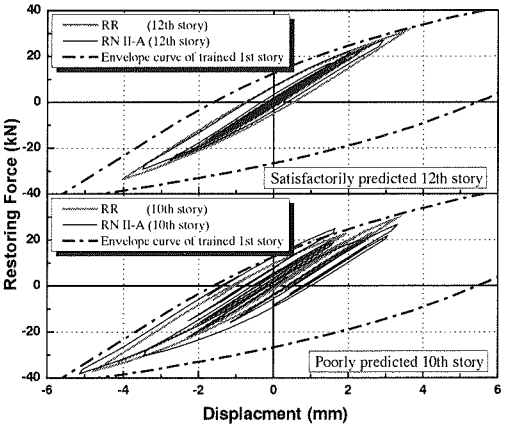

(3-A) 12-story model by RN II-A

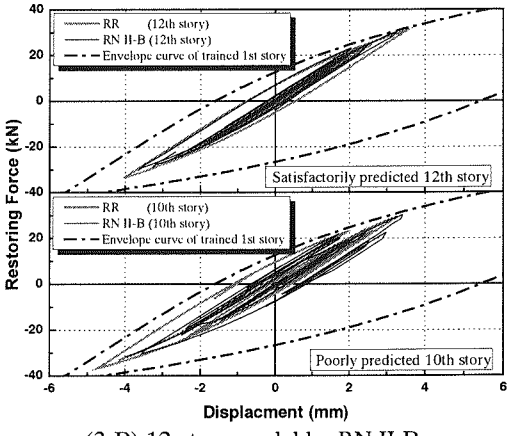

(3-B) 12-story model by RN II-B

Figure 10. Comparison of earthquake Response RR vs. RN (left: Input Layer A / right: Input Layer B)

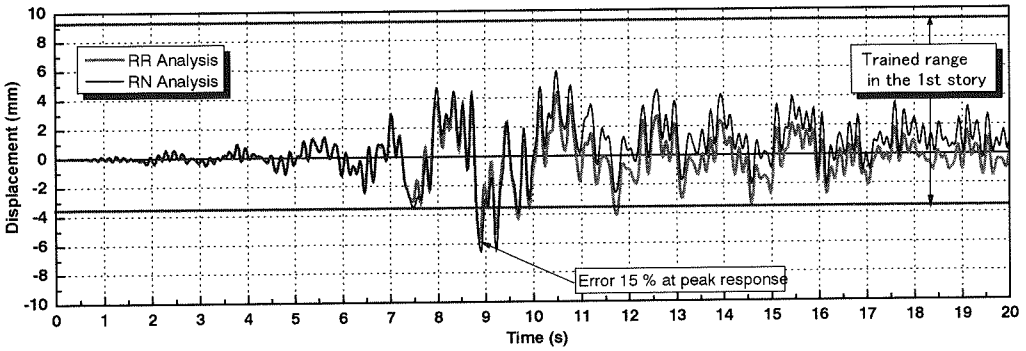

Figure 11. Comparison of response displacement RR vs. RN (Case RNII-B of 8-story model)

As can be found in Figure 10, the response is in general more successfully and stably reproduced under Input Layer B than under Input Layer A. Furthermore, the response is much better predicted when the predicted response falls within the range of the hysteretic loop of the trained first story ((2-B) vs. (1-B) and (3-B)). It should be pointed out, however, that that the maximum error at the peak response is approximately 15 % even in the worst case as shown in Figures 10 (2-B) and 11, and RNII-B shows the robust predictability in this study even when the number of members to be predicted increases. This result implies that the network with the normalization method II and the input layer B (i.e., RNII-B) can predict the response to some extent under extrapolation as well as under interpolation, although the interpolation may result in a better prediction.

SUBSTRUCTURE ONLINE TEST USING HYSTERETIC CHARACTERISTICS PREDICTED WITH NEURAL NETWORK

Specimens and loading system

To verify the applicability and the effectiveness of the proposed scheme in the substructure online tests, four sets of specimens (OT, SOT1, SOT2, and NSOT) are made and tested under different loading control. Table 4 shows the test parameters. Each specimen is a simple two-degree-of-freedom system representing the prototype structure shown in Figure 12(a), and each test part is, as shown in Figure 13, replaced with 2 sets of identical H-shaped steel sections. The specimens are all taken from a single

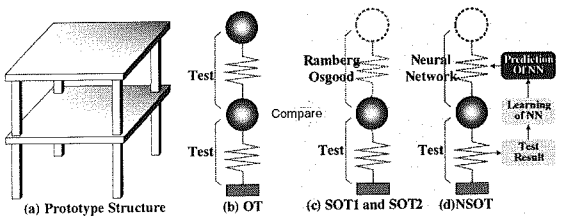

Figure 12. Test structures

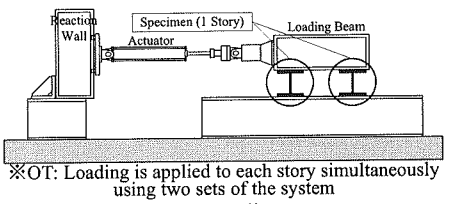

Figure 13. Loading system

Table 4. Test parameters

Test Name	1st story	2nd story
OT	Test	Test
SOT 1	Test	Ramberg-Osgood model (The hysteretic loop shape parameters are determined from the geometric size and material properties prior to test)
SOT 2	Test	Ramberg-Osgood model (The hysteretic loop shape parameters are determined considering test results of NSOT)
NSOT	Test	Predicted with neural network learning hysteresis of the first story during test

H-shaped steel member to minimize the test error associated with material uncertainties.

Specimen OT is tested to obtain a correct (or target) response to be compared with other test results. Each story is loaded using 2 sets of loading system shown in Figure 13. In specimen NSOT, a neural network that learns the load-deflection relationship in the first story is formed at every loading step, and the hysteretic loop in the second story is predicted using the network on real-time basis with on-going substructure online test. In the test, a combination of the normalization method II and the input layer B is used in the network. Note that the predicted restoring force at the current step i is fed back to define the input variables (2) and (4) shown in Table 1 in the subsequent computation step i+1, as is done in previously discussed numerical simulations. Specimens SOT1 and SOT2 are made based on a conventional substructure online test scheme, where the first story is characterized from the

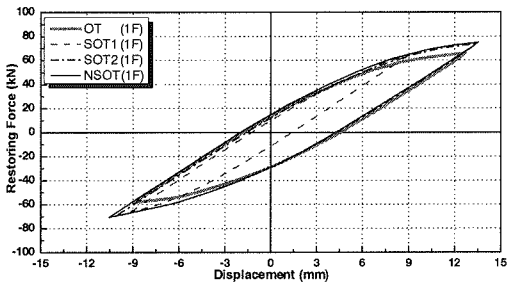

Figure 14. Envelope curves in the 1st story

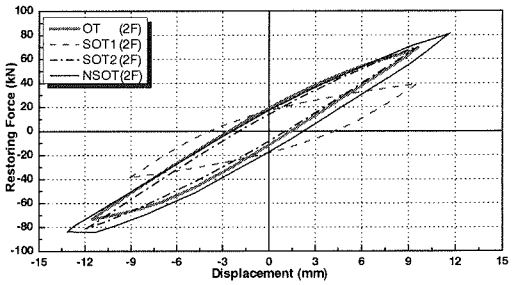

Figure 15. Envelope curves in the 2nd story

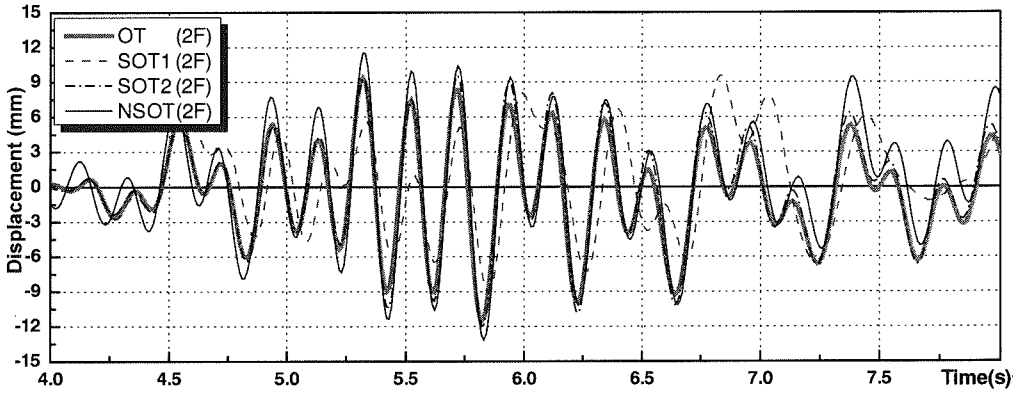

Figure 16. Comparison of response displacement in the 2nd story

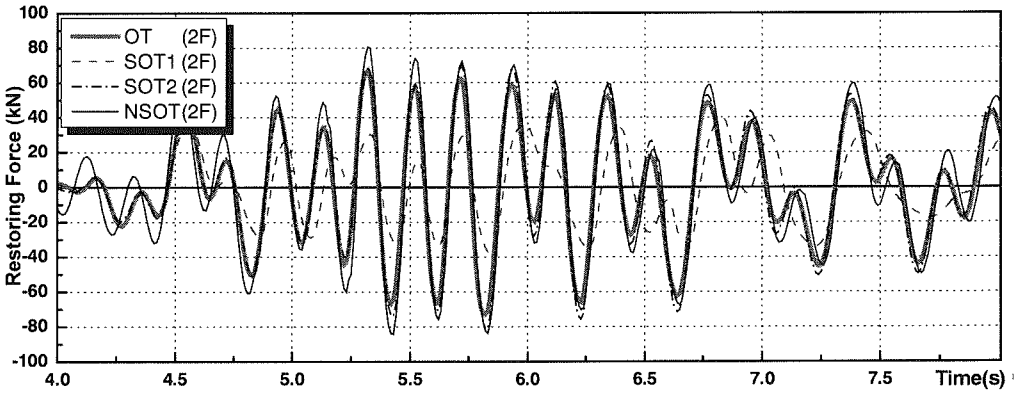

Figure 17. Comparison of restoring force in the 2nd story

loading test and the second story from a predetermined hysteretic rule. In this study, the Ramberg-Osgood model is employed for the second story. It should be noted that the shape parameters of the model are predetermined in SOT1 based only on the geometric size and material properties while they are determined in SOT2 considering the load-deflection curve obtained from the preceded NSOT results.

As is employed in the numerical simulations, the NS component of the Chiba-ken Toho-oki earthquake and the OS method are applied and the damping effects are neglected in the response computation.

Test results

Figures 14 and 15 show the envelope curves of response in the first and second story of OT, SOT1, SOT2, and NSOT. As can be found in the figures, NSOT and SOT2 satisfactorily reproduce the response of OT while SOT1 significantly differs from OT. It should be pointed out that a poor reproduction of response in SOT1 can also be found in the first story because the prediction error made in the second story significantly affects the response in the loading test story (i.e., first story). The precisely predicted hysteretic characteristics in the numerical simulation part, therefore, are most essential to successfully simulate the earthquake response of an entire structure.

Figures 16 and 17 show the time history of response displacement and restoring force. These results again show that NSOT as well as SOT2 can successfully reproduce the response of OT. Bearing in mind that the hysteretic shape parameters in SOT2 are determined from preceded test results while no shape parameters are needed prior to the loading test in NSOT, the proposed scheme has a major advantage over others because NSOT can simulate the correct response even if detailed structural information regarding the numerical simulation part of a structure is not available prior to the tests.

CONCLUSIONS

To establish the substructure online test technique using a real-time hysteretic modeling with a neural network, the formulation of network is investigated focusing on its structure, learning algorithm etc. and its validity and applicability are examined through both analytical and experimental investigations. The major findings obtained in this study are summarized as follows.

1) The structure of the neural network employed in this study can be applied to predict the hysteretic characteristics of structural members. In particular, the normalization method II proposed in this paper can significantly reduce the learning time and improve the prediction performance even if the number of data to be learned increases as the loading test progresses.
2) The neural network with input layer B shows generally more successful and stable response prediction than that with input layer A, even when the extrapolation is needed in predicting the hysteretic rule.
3) The substructure online test is successfully performed using the real-time hysteretic prediction with the proposed neural network, and its applicability is experimentally verified. In particular, although the restoring forces predicted by the network are repeatedly used as subsequent input data, the network is robust enough and does not accumulate prediction errors to terminate the test.
4) The conventional substructure online test (SOT1) does not successfully reproduce the correct target response (OT). The poor prediction performance is also found in the first story because the prediction error made in the predicted story (i.e., second story) significantly affects the response in the loading test story (i.e., first story). The other conventional test (SOT2), however, successfully simulates the behavior of OT because the hysteretic rules are determined considering the preceded test results of NSOT. The precisely predicted hysteretic characteristics in the numerical simulation part, therefore, are most essential to successfully simulate the earthquake response of an entire

structure.

5) The substructure online test using the scheme proposed in this study (NSOT) can satisfactorily reproduce the correct target response (OT). The proposed scheme therefore has a major advantage over others because NSOT can simulate the correct response even if detailed structural information regarding the numerical simulation part of a structure is not available prior to an online test.

ACKNOWLEDGEMENTS

The authors wish to thank Associate Professor Nobuhiro Yoshikawa, Technical Assistant Kayo Satoh, and Research Associate Yosuke Shimawaki at the Institute of Industrial Science, University of Tokyo, and Dr. Koichi Kusunoki of the Building Research Institute, for their valuable advice and contribution to this work. This study was partially supported by the Grant-in-Aid for Scientific Research by the Ministry of Education of Japan (Principal Investigator: Yoshiaki Nakano, Grant No. 08875101).

REFERENCES

1. Nakasima M, Ishida M, Ando K. Integration Techniques for Substructure Pseudo-Dynamic Test. *Journal of Structural and Construction Engineering* (Architectural Institute of Japan) 1990; **417**: pp. 107-117.
2. Tsutumi H, Sato K, Ando K, Ishida M, Ishii K, Iizuka M, Tagami J, Kato H, Yamazaki Y, Kaminosono T, Nakashima M. Pseudo Dynamic Testing Using Substructuring Techniques (Part 1 – Part 3). *Proceedings of the Eighth Japan Earthquake Engineering Symposium*, Tokyo, Japan, 1990; Vol. 2: pp.1935-1952.
3. Ichikawa H. *Application of Multilayer Feed-forward Neural Network to Nonlinear Analysis.* Kyoritsu Shuppann Co. LTD: 1993; pp. 29-30 (in Japanese).
4. Yang W, Nakano Y, Kusunoki K. Application of Neural Network to Substructure Online Test (Part 2: Comparison of BP and WL Algorithms, and the Effect of Input Layer Units on the Accuracy of Estimation). *Summaries of Technical Papers of Annual Meeting* (Architectural Institute of Japan) 1999; Vol. C-1: pp. 411-412.
5. Satoh K, Yoshikawa N, Nakano Y, Yang W. Whole Learning Algorithm of Neural Network for Modeling Nonlinear and Dynamic Behavior of RC Members. *Structural Engineering and Mechanics* 2001; Vol. 12, No. 5: pp. 527-540.
6. Hangai Y, Kawaguchi K. *Shape Analysis*. Baifukan Co. LTD: Tokyo, 1991. (in Japanese).
7. Yamamoto K. Modeling of Hysteretic Behavior with Neural Networks, and Its Application to Nonlinear Dynamic Analysis. *Journal of Structural Engineering* (Architectural Institute of Japan) 1992; Vol. 38A: pp. 85-94.
8. Joghataie A, Ghaboussi J, Wu X. Learning and Architecture Determination through Automatic Node Generation. *Proceedings of International Conference on Artificial Neural Networks in Engineering*, St. Louis, USA, 1995.
9. W. Yang, Y. Nakano, and Y. Sanada. The Application of Neural Network to Substructure Online Test and Learning Algorithm. *Proceedings of the Japan Concrete Institute* (Japan Concrete Institute) 2003; Vol. 25: pp. 1219-1224.